Available online at www.sciencedirect.com
SCIENCE DIRECT
Journal of Pharmaceutical and Biomedical Analysis 41 (2006) 811–819
JOURNAL OF PHARMACEUTICAL AND BIOMEDICAL ANALYSIS
www.elsevier.com/locate/jpba

Raman spectroscopy for tablet coating thickness quantification and coating characterization in the presence of strong fluorescent interference

Saly Romero-Torres [a], José D. Pérez-Ramos [b], Kenneth R. Morris [b], Edward R. Grant [c,*]

[a] *Department of Chemistry, Purdue University, West Lafayette, IN 47907, United States*
[b] *Department of Industrial and Physical Pharmacy, Purdue University, West Lafayette, IN 47907, United States*
[c] *Department of Chemistry, University of British Columbia, Vancouver, BC, Canada V6T 1Z3*

Received 3 October 2005; accepted 18 January 2006
Available online 24 February 2006

Abstract

We report a novel approach to the measurement of colored tablet coating thickness, which employs Raman spectroscopy with univariate and multivariate data analysis. Our results suggest that Raman sensing can serve as a viable non-invasive means to quantify tablet coating thickness in the presence of a fluorescent ingredient in the coating formulation (food colorant Alphazurine FG or D&C Blue No. 4). This study comparatively tests the advantage of several data transformation approaches, including mean centering, standard normal variate, and Savitzky–Golay smoothed second derivative as means of improving predictive models in the presence of fluorescence. By application of the partial least squares (PLS) calibration algorithm to establish optimum covariance between transformed spectral data and measured tablet coating thicknesses, we have been able to create predictive models with calibration errors as small as 4 μm for a training set that spans colored coating thicknesses from 50 to 151 μm.

Keywords: Raman spectroscopy; Near infrared spectroscopy; Film coating; Fluorescence

1. Introduction

1.1. Raman spectroscopy

Raman spectroscopy has attracted substantial attention in the global pharmaceutical industry over the past few years as a novel analytical tool for process control monitoring [1]. This analytical method provides a convenient means to register the fundamental vibrational spectrum of a solid or liquid sample. It conveys this information by means of the inelastic scattering of monochromatic radiation [2]. Such measurements can be performed non-invasively and require little or no sample preparation. Spectra can be collected remotely by means of fiber optics, and analyzed by sophisticated pattern recognition techniques to obtain composition information for complex mixtures [3].

Reliable control of pharmaceutical manufacturing operations requires knowledge concerning physical as well as chemical characteristics of a drug formulation over the course of all its unit operations. For this reason, pharmaceutical researchers have recognized the utility of non-destructive Raman methodologies as a potential tool for application in advanced process analysis schemes aimed at determining tablet drug content [4], and monitoring polymorphism transitions [5,6]. Nevertheless, despite its apparent advantages, Raman spectroscopy has found only limited use in practice for these and other applications, owing in part to the problem of fluorescence, especially encountered for colored samples under visible excitation. Other problems encountered with colored samples relate to the possibility of photochemistry and photoinitiated thermal decomposition [1].

Interfering luminescence, which can mask the Raman spectrum of vibrational shifts, is produced in many systems by the spontaneous emission of photons from low-lying excited electronic states. This effect occurs in a sample whenever the frequency of the excitation laser coincides with a transition energy from the ground to an electronically excited state. The fluorescence signal, when present, is usually much stronger than Raman scattering. To avoid this problem, spectroscopists commonly employ excitation sources in the near infrared region (NIR), where the illuminating source has insufficient frequency energy to reach most fluorescence-producing excited electronic states.

In considering the use of Raman spectroscopy as an analytical sensor for pharmaceutical or food industry process monitoring,

* Corresponding author. Tel.: +1 604 822 2471; fax: +1 604 822 8710.
E-mail address: edgrant@chem.ubc.ca (E.R. Grant).

0731-7085/$ – see front matter © 2006 Elsevier B.V. All rights reserved.
doi:10.1016/j.jpba.2006.01.033

the analyst should be aware, however, that certain substances do fluoresce when irradiated with NIR light sources. Common near infrared fluorescent substances include iron oxide, which is often utilized in tablet coatings or incorporated in the tablet core as a colorant [5] and food colorants, such as Alphazurine FG. The use of these or other NIR fluorescent materials can be perceived to limit the utility of Raman as a tool to support drug research, development and quality control. Several mathematical corrections have been employed to correct for fluorescent background. Typically, one simply subtracts a representative pure background from the spectrum of interest. Alternatively, spectra can be corrected by subtraction of individually fitted background functions. Both of these correction methods can add noise, and, especially in the case of individualized background corrections, can introduce uncontrolled variations that interfere with multivariate analysis [7].

1.2. The importance of monitoring tablet coatings

Film coating is often employed as final and separate operation in the manufacturing of pharmaceutical or nutritional oral solid dosage forms. A coating barrier offers advantages to the consumer and in the pharmaceutical manufacturing process. Perhaps most important among these is the function of controlling the release of the API into the body. Coatings can also provide physiological advantages by reducing irritation associated with the exposure of the stomach to high concentrations of medications. Tablet film coatings play a basic role in improving product visual appearance. They are commonly employed to improve tablet swallowability. An intact coating can mask unpleasant tastes and odors, and protect against water and oxygen, which can degrade the API.

1.3. Use of aqueous based film coating

The use of aqueous based tablet film coating has become more popular in recent years. This involves the addition of a film-forming polymer layer onto a substrate tablet surface. In traditional pharmaceutical applications, the coating consists of polymer, plasticizers and colorants, which are needed to achieve the desired properties in the final dosage form. The polymer and the plasticizer are usually dissolved in the aqueous coating solution in which the colorants can be dissolved or dispersed.

1.4. Colorants in film coatings

The coloring of pharmaceutical dosage forms is extremely useful for identification during manufacturing and distribution. Many patients rely on color to recognize the prescribed drug and proper dosage. Since film coatings are relatively thin, small differences in film thickness may induce considerable color variations in the tablet surface.

1.5. Means of monitoring film coating

Because the quality and quantity of coating can influence the dissolution and bioavailability of a drug, coating characteristics constitute critical and regulated parameters, which must be assessed by integrity and uniformity analysis. A number of instrumental methods have been introduced and evaluated as means for coating process monitoring. These methods range from liquid chromatography [8] to various non-invasive spectroscopic probes. One approach that has been favored for its rapid throughput is laser-induced breakdown spectroscopy (LIBS), particularly as a means for assessing coating thickness uniformity [9]. The main drawback of this method is its destructive nature [10]. Near infrared spectroscopy has also been employed, mainly for coating quantification [11–13], but uneven distribution of standards coating from tablet-to-tablet have caused imprecision in the calibration and validation models using this technique. The direct measurement of film coating thickness using sectioning and microscopy gives reasonably accurate results, but this technique is laborious and impractical for real-time process monitoring.

Many film coating characterization and quantification procedures have proven difficult and irreproducible in part because coating agents are often found unequally distributed over the tablet surface. Nevertheless, the measurement of tablet-to-tablet coating variations has been suggested as an important means of characterizing different coating process stages. Coating parameterization can thus be regarded as a source of information on outcomes that can provide feedback for coating process mechanism design [14], and serve as a touch point for real-time control leading ultimately to fundamental improvements in product performance and reliability. Previous work from our group has demonstrated the feasibility of Raman spectroscopy combined with multivariate analysis as a technique to monitor tablet-to-tablet coating variability [15]. In that work, we correlated coating time with the multivariate characteristics of Raman spectra observed for a batch of Sulfanilamide tablets that were systematically coated with a clear aqueous hydroxypropyl methylcellulose (HPMC) polymer solution. Though a separate study has established a linear relation between coating time and coating thickness for the same batch of tablets [16], we did not calibrate directly to thickness in our initial investigation of tablet-to-tablet coating variability.

1.6. Application of Raman spectroscopy to coating characterization

In the present work, we have performed a series of univariate and multivariate analyses to understand and characterize the simultaneous scattering and absorbance phenomena in Raman spectroscopy due to fluorescent coatings. We have also explored the possibility and limitations of using Raman spectroscopy as an alternative method to characterize and quantify colored film coatings in tablets. Our results suggest that Raman spectroscopy combined with appropriate data-pretreatment can serve as an effective tool for pharmaceutical coating quantification under fluorescent conditions and at the same time convey information related to the control of coating process stages.

2. Experimental

2.1. Materials

Tablet core formulation: Sulfanilamide (purum, 98.0%; FLUKA, Buchs SG, Switzerland, and Riedel-de Haën, Seelze, Germany), microcrystalline cellulose (Avicel^{TM} PH-200 NF; FMC, Newark, DE), lactose anhydrous for direct compression (Sheffield Brand Lactose N.F; Quest International, Chicago, IL), and magnesium stearate (Witco Corporation, Houston, TX) were sieved through a #30 US standard sieve to make the directly compressible formulation for the tablets.

Coating formulation: hydroxypropyl methylcellulose (HPMC, Methocel^{TM} E3 grade; Dow Chemical Company, Midland, MI), polyethylene glycol 6000 (USP/EP; Dow Chemical Company), D&C Blue No. 4 dye were used as received.

2.2. Tablet manufacturing

2.2.1. Compression

All tablet ingredients were blended in a Tote bin blender. Tablets containing 30% (w/w) microcrystalline cellulose, 50% (w/w) lactose anhydrous, 20% (w/w) Sulfanilamide and 0.2% (w/w) of total weight for magnesium stearate were compressed with 7/16″ in standard round concave punches to a target weight of 480 mg on a Stokes 16-station B2 tablet press (FJ Stokes Machine Company, Philadelphia, PA).

2.2.2. Coating solution

An aqueous based coating solution was prepared, consisting of 10% (w/w) hydroxypropyl methylcellulose and 1% (w/w) polyethylene glycol. The polyethylene glycol was added to 7 l of 60 °C distilled water. After the polyethylene glycol was dissolved, hydroxypropyl methylcellulose was slowly added while mixing continued for 20 min to fully disperse the polymer. The D&C Blue No. 4 dye was finally added and mixing was continued for an additional 15 min. The solution was removed from the heat and allowed to sit for at least 12 h before use to hydrate the polymer.

2.2.3. Coating apparatus

Film coating experiments were performed in a 24-in diameter Accela–Cota pan coater using a single two-phase coating spray nozzle. The inlet air temperature was controlled with a heat exchanger at 60 °C during the coating operation. The pan speed was maintained at 12 rpm during the coating stage of each experiment.

2.3. Methods

Each coating experiment began with 7 kg of tablets in the pan coater. The tablet bed was allowed to warm up for 15 min prior to the coating operation. The coating solution was applied at a rate of 50 g/min using a single two-phase nozzle placed 6 in from the cascading bed of tablets. The inlet air temperature was controlled to 60 ± 1 °C, and the outlet air temperature stabilized at approximately 42 °C throughout each coating experiment due to evaporative cooling. The pan speed was maintained at 12 rpm during the coating operation. At the end of the coating step, the pan speed was reduced to 8 rpm and the heat exchanger was turned off. The coated tablets were allowed to cool down for 20 min. Tablet samples of approximately 100 g were collected at 20-min intervals during the coating experiments. Room temperature was maintained between 21 and 23 °C and the relative humidity was maintained between 19 and 24%, respectively.

2.3.1. Tablet weight

Following each coating experiment, the individual weights of 100 tablets for each sample coating time (20 min intervals) were measured on a Mettler-Toledo AG104 analytical balance (Mettler-Toledo, Columbus, OH). The average weight and standard deviation were calculated from the individual weights.

2.3.2. Tablet dimensions

After each coating experiment, we determined face thickness for 100 tablets from each coating-time sample using a digital micrometer (Mitutoyo Digimatic Outside Micrometer, Mitutoyo America Corporation, Aurora, IL).

2.3.3. Tablet film thickness

We estimated the thickness of the film coat on individual tablets from a measurement of tablet dimensions using the digital micrometer. We took the film thickness for uncoated tablets to be zero and ascribed a tablet dimensional change entirely to the film solids deposited on its surface. We measured one hundred tablets for each 20-min coating interval and averaged these values to determine a representative coating thickness and standard deviation for each coating-time population.

2.3.4. Raman spectral acquisition

We acquired spontaneous Raman spectra using an adjustable probe, connected by a 5-m fiber-optic umbilical to a mobile console (RP-1 Identification System, Spectracode Inc., Purdue Research Park, West Lafayette, IN). The average coating thicknesses for the tablet calibration and validation sets were: 23, 50, 80, 93, 106, 139 and 151 μm. Thirty tablets per coating interval were analyzed in triplicate over three different areas of each tablet. Tablets were rotated at 100 rpm during measurement to obtain a well-averaged, representative spectrum [20]. The Raman spectral acquisition exposure time was 0.15 s and the excitation source was a 787 nm diode laser with a power of 1 W. The instrument resolution was 25 cm^{-1} (100 μm slit dispersed by 600 g/mm grating and collected by a 256 × 1024 pixel CCD), well matched to the laser output bandwidth of 2 nm. The probe head of our instrument employs holographic optics to collect and filter the scattered radiation. The 5 mm depth of field of this instrument eliminated the need for precise tablet alignment.

2.4. Model creation

2.4.1. Univariate analysis

To analyze the effect of fluorescence on the characterization of tablet coatings by Raman scattering we developed different mathematical representations of a feature property of the tablet

spectrum as a function of measured coating thickness. These representations were obtained by creating a *Y–X* data set relating the baseline adjusted and pretreated Raman intensities (*Y*) of a characteristic API peak to the corresponding coating thickness of the tablet (*X*). These data sets were fit to exponential functions that follow the Beer–Lambert absorption law. Furthermore, each of these univariate calibrations data sets was compared with a univariate calibration of a matching tablet set with the same tablet and coating formulation, but without the blue fluorescent dye.

2.4.2. Multivariate analysis

Multivariate models correlating Raman spectral data with coating thicknesses (μm) were constructed using, partial least squares (PLS). The PLS method functions in general to yield a multidimensional model capable of predicting a set of dependent variables, *Y*, by means of a basis set of independent variables, *X* [17]. In the case of our study, these variables consist respectively of *coating thickness* in microns and *Raman intensity units* in the wave number space of the Raman shift spectral window. Our calibration model was based upon a set of 160 tablets, which were selected in order to obtain a representative population for each tablet coating thickness. A separate set of 80 tablets was used to test the correlation. The algorithm used to achieve this correlation is based on a non-linear iterative partial least squares (NIPALS) decomposition, wherein sets of orthogonal factors or latent variables (LVs) are calculated simultaneously using the covariance between the dependent and independent variables [18,19]. These factors then model the Raman data (X-block), and, at the same time, correlate it with coating thickness (Y-block). By this algorithm we expressed the coating thickness as a linear function of Raman intensities. PLS models and Savitzky–Golay second derivative smoothing [21] were carried out using the Unscrambler software (7.6 SR-1, Camo Technologies, Woodbridge, NJ). Data preprocessing (mean centering and standard normal variate) were carried out using Microsoft Excel 2000.

3. Results and discussion

3.1. Data examination and preprocesses

The system under study exhibits mass fractions of coating solids that range from 0 to 10%, as calculated from weight gain during the pan coating operation. This corresponds to coatings as thick as 150 μm in the biconvex tablet face region. By inspecting the mean centered (MC) spectra of the tablets in the calibration set with coating thicknesses of zero, Fig. 1, we can easily identify a set of API Sulfanilamide Raman bands. These appear with characteristic Raman shifts representing the ring stretches and symmetric SO_2 stretch at 1630 and 1177 cm^{-1}, respectively. Spectral data for other tablets encased in coating agent with Blue No. 4 show that the relative intensity of these API bands decreases drastically with coating thickness preventing coating characterization by peak height alone.

In order to correct for baseline shifts, which may introduce irrelevant variation during multivariate analysis, the MC spectral

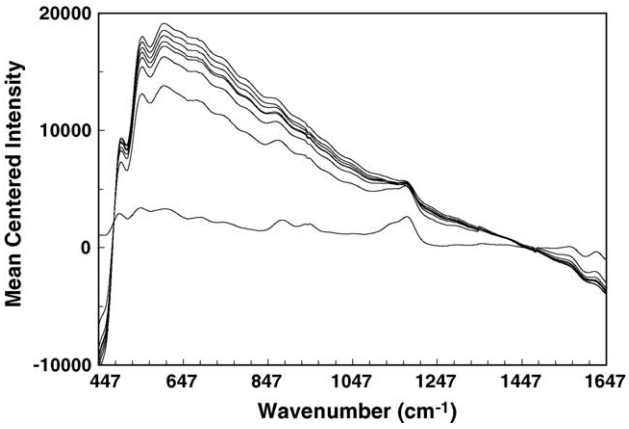

Fig. 1. Mean centered Raman spectra showing ring stretch and symmetric SO_2 stretch at 1630 and 1177 cm^{-1}, respectively, which corresponds to the API Sulfanilamide Raman bands.

data was also autoscaled by dividing each spectrum by its respective standard deviation, Fig. 2. This mean centering autoscaling algorithm is commonly known as standard normal variate (SNV) normalization. The use of the SNV normalizing algorithm offers a means to correct the intensity changes (multiplicative effect) by casting the spectral data variance about a zero mean, which emphasizes its characteristic features and scales the waveform to a unit variance:

$$\mathrm{SNV}_{\mathrm{Data}} = \frac{Y_{\mathrm{Data}} - Y_{\mathrm{Average}}}{Y_{\mathrm{STDEV}}}$$

This algorithm shifts the baseline by means of an individualized correction [22,23]. Another pretreatment that could have been employed to correct for multiplicative effect is multiplicative scatter correction (MSC) [24]. The data processing MSC algorithm compares spectra associated with each different coating thickness to a reference spectrum that is created from the average of all spectra. Even thought the MSC method was demonstrated to accomplish the same level of correction as the SNV data pretreatment in a previous coating thickness study [15], the individualized spectral correction of SNV is simpler to execute. For an elegant comparison between these two pretreatments the reader is referred to Ref. [25].

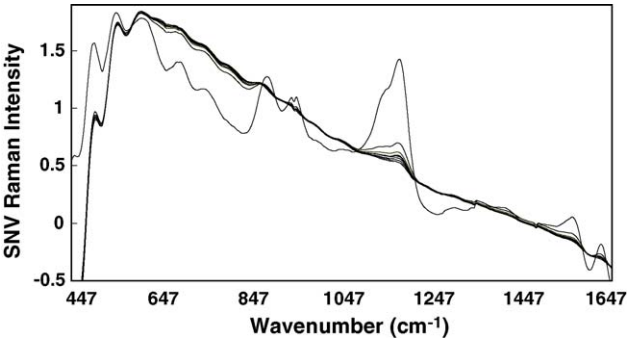

Fig. 2. SNV Raman spectrum of HPMC and Blue No. 4 coated tablets with different coating thicknesses. The symmetric SO_2 stretch at 1177 cm^{-1} from the Sulfanilamide active ingredient decreases exponentially as thickness increases. In this region, the traces reading from top to bottom correspond to coating thicknesses of 0, 23, 50, 80, 93, 106, 139 and 151 μm.

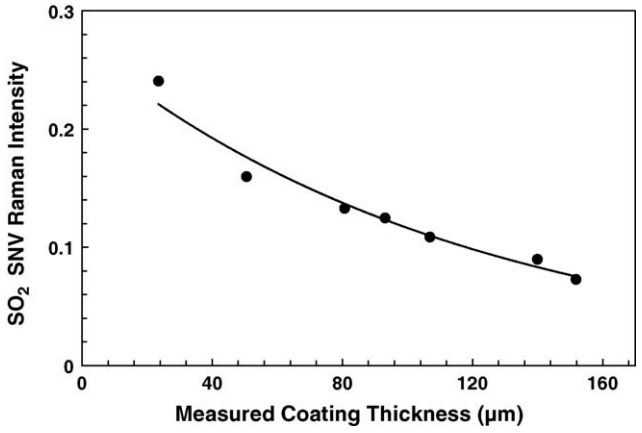

Fig. 3. Univariate calibration and outlier plot showing the relationship between intensity and coating thickness with reference to the symmetric SO_2 stretch sulfanilamide Raman band at 1177 cm^{-1}. Curvature here illustrates the non-linear relationship between this Raman feature and coating thickness in our tablet set.

The spectral variations of MC and SNV transformed data were further emphasized by employing an additional step in which we smoothed the data by regressing local data points or windows to a cubic polynomial and then calculating the second derivative of this fitted polynomial. This technique of smoothing differentiation is called Savitzky–Golay second derivative (SGSD). In our analysis, the windows were of 57 and 34 cm^{-1}, or 11 and 7 pixels, respectively. All of these data transformations provided the input for the construction of a series of univariate and multivariate calibration models.

3.2. Univariate calibration analyses

To verify the possibility of univariate analysis and determine the linearity of our data, we created a series of plots showing the intensity decrement of active Raman bands as coating thickness increases depending on the data pretreatment. We utilized the symmetric SO_2 stretch band baseline adjusted intensity at 1177 cm^{-1} for this purpose. The univariate calibration of the MC data set included tablet calibration sets from 0 to 151 μm. The exponential fitted calibration equation, for this set, gave a correlation factor, R^2, of 0.89. As a matter of exploring better approaches for univariate calibration, we also constructed a second univariate calibration curve with the SNV baseline adjusted calibration set. In order to obtain a reasonable univariate calibration with the SNV 1177 cm^{-1} adjusted intensity, we omitted tablets from uncoated sample set. When the uncoated samples were included, the difference in their baseline compared with the baseline for fluorescent tablets produced a problematic double-exponential correlation between the feature intensity and coating thickness. By contrast, univariate calibration without the uncoated standards returned a single-exponential fall in the symmetric SO_2 stretch intensity as a function of the tablet coating thickness, which fits with the Beer–Lambert law for radiation absorption. This is depicted in Fig. 3 and described by the following equation:

$$P = P_0 e^{-XBC}$$

Table 1
Differences between the measured and predicted values for the SNV univariate coating thickness calibration model

Coating thickness (μm)	Bias from univariate calibration model (μm)
23	17
50	−13
80	−9
93	−3
106	−12
139	4
151	6

where P is the Raman feature intensity at 1177 cm^{-1}, P_0 the unattenuated scattered light intensity, X the molar absorptivity, which is wavelength dependent, C the concentration of absorptive species and B is the light path. Since for this study the concentration density of the absorptive blue dye in the coating solution and its absorption coefficient can be assumed to be constant, we recognize the path length as the independent variable. The SNV univariate calibration model fit an exponential equation:

$$P = 0.27\, e^{-0.0084B}$$

which gives an R^2 of 0.97 for the calibration data set and yields a root mean square of error (RMSE) of 10 μm, when used to calculate the coating thicknesses of the validation set.

We have also explored the adjusted intensity of the ring stretch at 1630 cm^{-1} as a possible calibration variable. This ring stretch presents the same exponential behavior as the SO_2 band intensity, but with lower signal-to-noise ratio and thus lower correlation and higher RMSE. The same variables were used to construct a univariate model that employs data pretreatments consisting of SNV in conjunction with SGSD with a window of 52 cm^{-1}, but this data pretreatment yields lower correlations, 0.93 and 0.90 for the calibration and prediction set, respectively.

Univariate calibration using the SNV 1177 cm^{-1} adjusted intensity Raman feature from the tablet bulk, provides a viable means for coating thickness quantification. However, improved correlation in the calibration model and lowered errors in future predictions will require a larger number of samples. This will be especially necessary in the thickness range from 23 to 50 μm, where the exponential calibration curve is steepest. Here, the difference between the measured and predicted values of the two tablet sets is higher than values obtained for the rest of the calibration set (Table 1). Introducing more tablet standards in this region of the calibration curve should help the model better cover the range.

3.3. Multivariate calibration analysis

Multivariate calibration analysis offers the advantage of using calibration vectors instead of single wavelength. This often yields more robust calibrations since multidimensional vectors carry more spectral information to correlate with the dependent variable of interest. In order to understand how our data behave in the new reduced data space created by the PLS anal-

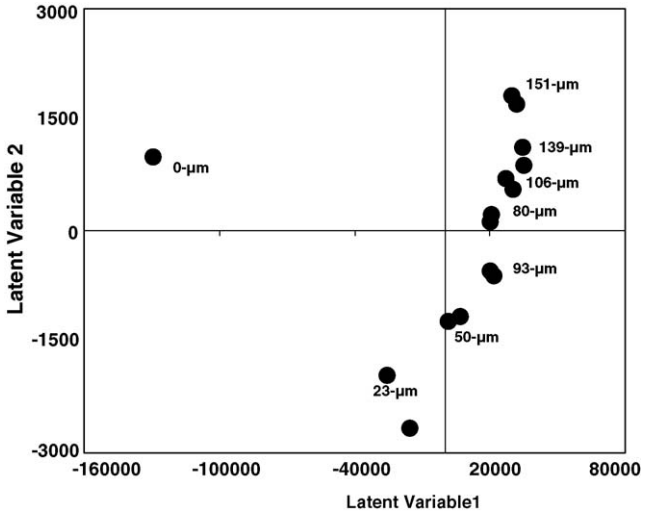

Fig. 4. Scores plot for the SNV Raman spectra (calibration and validation samples). The greatest discrimination between samples is observed between the coated vs. uncoated samples. The next greatest discrimination is given by the coating thickness increments.

ysis, we started by examining the plot of weighed factors also known as a Scores plot [18]. For the simplest of these models, we used the MC data and plotted all of the different coating thicknesses, including the tablet set without coating. As we can observe in Fig. 4, this plot presents a negative correlation between two groups. The first LV discriminates between the coated and uncoated tablets, whereas the second LV describes coating thickness increments. This can be clearly visualized in the ascendance of the scores values from the different tablet sets along the second LV as the coating thickness increases. To emphasize the variance correlated with coating thickness quantification in the first LV, we removed the uncoated tablets from the reduced data space. With this modification the coating thickness variance becomes well described by the first LV.

We first constructed a PLS predictive model using the MC spectral data and the tablet sets from 23 to 151 μm. Our study suggests that for this model we should see the most improvement with two LVs, since the incorporation of a third yields no significant decrement in the residual *Y*-variance plot [17,26]. This model gives calibration and prediction correlations of 0.97 and 0.99, respectively, and root mean square of errors for calibration and prediction (RMSEC and RMSEP) of 8 and 5 μm. The further introduction of SGSD transformation to the MC data did not improve the PLS model. By comparing these correlation factors with the ones derived for the univariate calibration curve constructed on the basis of the MC and SNV Raman data transformations, we can conclude that the multivariate predictive models represents a significant calibration improvement.

As we did for the univariate analysis we decided to create prediction models based on the SNV pretreated data. The first of the SNV models included the tablet sets from 23 to 151 μm, and used only one LV. This model gave correlations of 0.95 and 0.93 with RMSEC and RMSEP of 12 and 15 μm. Since the data in the range 50–151 μm resembles a more linear model, the thinnest and thus least precisely determined 23 μm sample set was further

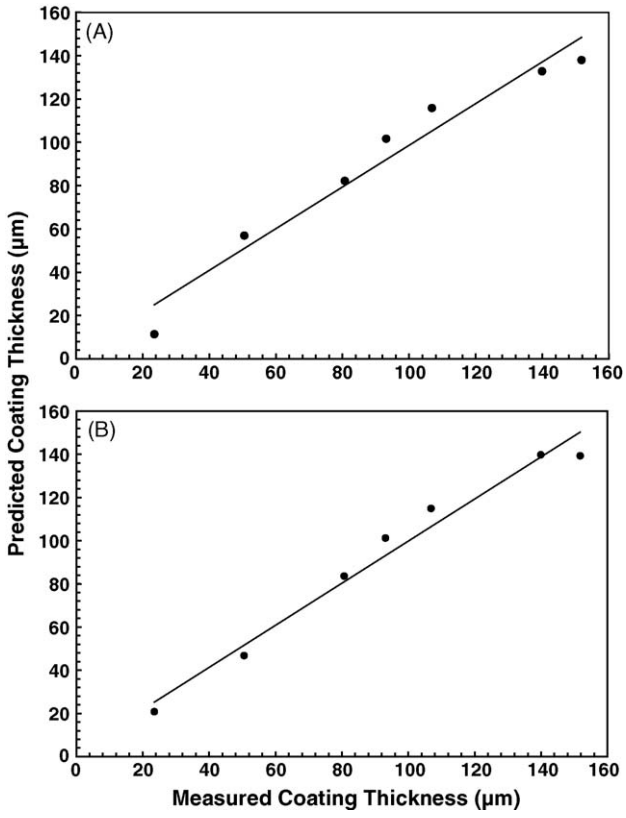

Fig. 5. Calibration (A) and prediction (B) variance regression model for SNV–SGSD Raman. This model uses two latent variables to describe the exponential relationship between SNV Raman intensity and coating thickness (μm).

eliminated from the reduced data space to improve the calibration. By doing this we obtained correlations of 0.97 and 0.98 with RMSEC and RMSEP of 8 and 7 μm, which presents a significant improvement over the model that contains the 23 μm training set.

In order to maximize the SNV spectral differences between tablet sets, we employed SGSD pretreatment with a moving window of 34 cm^{-1}. Using this data we built a two LV model by using the tablet sample sets from 23 to 151 μm. This model yields correlations of 0.98 and 0.97 for the calibration and validation regressions as well as RMSE of 6 and 9 μm for calibration and prediction, Fig. 5. Again, by removing the 23 μm samples from the training set and by changing the moving window to 57 cm^{-1}, which corresponds to the full width at half maximum of the Sulfanilamide feature at 1630 cm^{-1} [27], we were able to greatly reduce the error values to 4 and 6 μm for calibration and validation, respectively. This last model yielded correlation values of 0.99 and 0.98 for calibration and predictions. The removal of the 23 μm sample set limits the range of coating thickness prediction to 50–151 μm, but yields an accurate measure for samples expected to fall within this linear range of coating thickness variation. A summary of all calibration models and their respective goodness of fit can be found in Table 2. All of our multivariate models used the spectral variables from 386 to 1890 cm^{-1}.

These results show that Raman spectroscopy combined with multivariate analysis offers a non-destructive alternative to con-

Table 2
Variation of univariate and multivariate calibration with respect to data transformation

Calibration method and thickness range (μm)	Calibration algorithm	Pretreatment	Number of LV's	Calibration correlation	RMSE calibration (μm)	RMSE prediction (μm)
Univariate (23–151)	Regression	SNV	N/A	0.97	9	10
Multivariable (23–151)	PLS	MC	2	0.97	8	5
Multivariate (23–151)	PLS	SNV	1	0.95	12	15
Multivariate (50–151)	PLS	SNV	1	0.97	8	7
Multivariate (23–151)	PLS	SNV–SGSD	2	0.98	6	9
Multivariate (50–151)	PLS	SNV–SGSD	1	0.99	4	6

ventional analysis for determining tablet coating thicknesses, even in the presence of a strong fluorescent interference such as Blue No. 4, provided that care is taken in data pretreatment and that the desired quantification limits fall within the applicable interval.

For all of our PLS models, we have verified the *Y*-residuals distribution to obtain errors of prediction and calibration. The error distribution in the models is random against predicted values, which suggests no systematic error and no outliers [26].

3.4. Sources of error

Errors of calibration and prediction can be attributed to several factors. The main limiting factor can likely be ascribed to the fact that only 20 tablets were analyzed by Raman per coating thickness, whereas 100 tablets were used to calculate the average coating thickness value that was used as the Y matrix in the PLS analysis. We would expect accuracy to improve if we used a larger number of tablets to calculate a measured average coating thickness in keeping with the number of tablets measured with the digital micrometer.

Another important source of error is the possible tablet-to-tablet coating thickness inhomogeneity present in each of the calibration and validation tablet sets. This inhomogeneity leads to high standard deviations between tablets when calculating the average coating thickness value for each 100 tablet sets (Table 3). Another factor limiting the accuracy of the PLS regression for the validation relates to the number of tablets that were sampled to validate the prediction model. This was half the number used to construct the calibration set. Thus, our validation set under-represented and perhaps under-sampled. This may be especially the case for the sample sets with a nominal coating thickness of 23 and 50 μm, where narrower intervals of coating time and a greater number of validation samples may be required to characterize the exponential behavior in the steeper region. Finally, the lower signal-to-noise ratio for Raman features in fluorescent samples contributes to the quantification errors, especially when a non-representative calibration and validation set are created.

3.5. Fluorescence characterization

To gain more understanding of our films, we examined our tablets visually and under the microscope to look at the morphology of the coating surfaces. In tablets with the thinnest 23 μm coating, we found inhomogeneous regions of coating density, underlining the importance of our representative sampling technique, which averages over the tablet surface [20]. These inhomogeneities can also be related to the extent of steepness in the negative exponential behavior of our Raman signal versus the coating thickness of the tablet in the early stages of coating process. In an ideal limit, this coating morphology presents two surface transmission domains in the same tablet one with fluorescent signal and one without. This difference between domains can be attributed to the coating process, the physical relationship between the properties of the coating material and the tablet surface as well as the optical properties of the coating material.

We further studied the effect of fluorescence by examining spectral differences within tablets from the same set. To measure these spectral differences, we analyzed all coating thicknesses

Table 3
Coating thickness standard deviation for measured tablet sets

Coating time (min)	Face film thickness (μm)	Face film thickness standard deviation (μm)	Raman spectral standard deviation (arb. units)
0	0	7	13.2
20	23	9	5.81
40	50	11	4.44
60	80	10	3.59
80	93	14	4.42
100	106	10	3.54
120	139	9	2.96
139	151	12	2.96

The film thickness standard deviation values were estimated based on the tablet dimension measurements using a digital micrometer. The Raman spectral standard deviation, which measures the quality of spectral smoothness, presents a systematic pattern, which is inversely proportional to the fluorescent coating thickness.

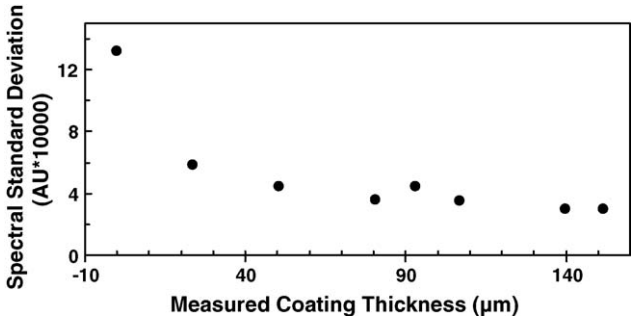

Fig. 6. As the coating thickness increases, the spectral standard deviation decreases exponentially, reflecting the spectral homogeneity caused by the peak masking due to fluorescence.

including 0 μm by measuring 60 tablets per coating thickness at five different points on each tablet, and then averaging these five points. The standard deviation for each tablet set was determined by calculating the standard deviation for each SNV–SGSD pixel intensity and then averaging these values. When we plot these averages against coating thickness, we find a negative exponential, which suggests another factor that is directly related to the fluorescent dye in the coating agent, Fig. 6. The exponential standard deviation decrement arises from the shift in the baseline, and the more uniform masking of Raman spectral features for thicker coatings. This phenomenon produces more homogeneous spectra and thus lowers the spectral standard deviation among tablets from the same set. Thus, standard deviation suppression can also be contemplated as an indirect calibration variable for fluorescent samples.

3.6. Comparison of dyed with non-dyed tablet coatings

By reference to spectra obtained in earlier work, we can characterize spectral differences between fluorescent tablets and tablets prepared with the same core and coating formulation but without the addition of the fluorescent agent. From this comparison we can conclude that the majority of the spectral background fluorescence arises from the inclusion of the blue dye in the coating solution and not from the core formulation. This can be confirmed by reference to Fig. 7, which presents the decrement in the SO_2 peak intensities versus coating thickness (μm).

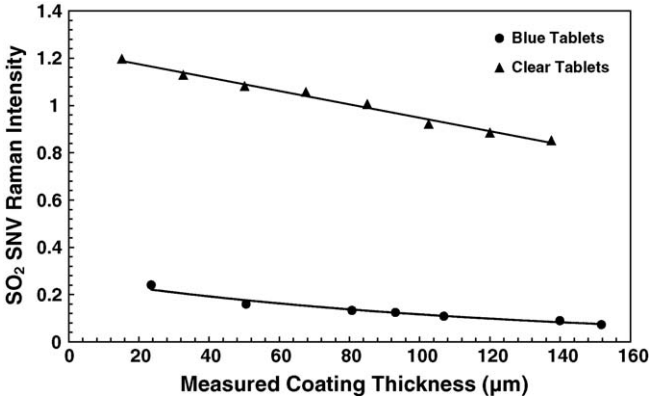

Fig. 7. Fitting for SO_2 1177 cm^{-1} corrected baseline intensity vs. tablet coating thickness; the circles represent the fitting for tablets with fluorescent agent and the triangles represent the set without fluorescent coating. The clear tablet set presents a linear calibration curve with an R^2 of 0.98.

4. Conclusions

Raman spectroscopy used in conjunction with the PLS algorithm, offers a promising means for creating predictive tablet coating thickness quantification models, even in the presence of a strong broad-band fluorescence interference, as that presented by Blue No. 4. A single-variable calibration derived from the Sulfanilamide symmetric SO_2 stretch band at 1177 cm^{-1} demonstrates the non-linear nature of this band intensity versus the coating thickness. This non-linearity is mainly attributed to the fluorescent dye that is present in the tablet coating solution. Taking into account this non-linearity, we have characterized several coating thickness calibration methods. These methods include: univariate calibrations using mean centered and standard normal variate transformations and multivariate calibration using a partial least squares calibration model with various data transformations. The best calibration model combines the SNV with SGSD preprocessing and employs only a single latent variable. This model shows high validity when confined to coating thicknesses interval from 50 to 151 μm. Thus, while this last model yields the lowest root mean square error of calibration and prediction, it limits the analytical working range to a region in which there is an apparent linear relationship between the coating thickness and the Raman spectral data. Better accuracy in univariate analysis will require more standards of different thicknesses representing the early stages of coating, which reflecting the steepest part of the exponential relationship between the Raman intensity and fluorescent tablet coating thickness.

Acknowledgments

The authors gratefully acknowledge Pradeep N. Perera for help in obtaining bright-field microscope images. This study was supported by a grant from e-Enterprise Center of Purdue University's Discovery Park and the NSF Center for Pharmaceutical Processing Research (CPPR).

References

[1] A.C. Williams, Handbook of Raman Spectroscopy: From the Research Laboratory to the Process Line, Marcel Dekker, Inc., New York, NY, 2001.
[2] J. Laserna, in: R.A. Meyers (Ed.), Encyclopedia of Analytical Chemistry, John Wiley & Sons, Ltd., 2000, pp. 13019–13057.
[3] C.J. Strachan, D. Pratiwi, K.C. Gordon, T. Rades, J. Raman Spectrosc. 35 (2004) 347–352.
[4] I. Jedvert, M. Josefson, F. Langkilde, J. Near Infrared Spectrosc. 6 (1998) 279–289.
[5] L.S. Taylor, F.W. Langkilde, J. Pharm. Sci. 89 (2000) 1342–1353.
[6] G. Fini, J. Raman Spectrosc. 35 (2004) 335–337.
[7] J.M. Shaver, Handbook of Raman Spectroscopy: From the Research Laboratory to the Process Line, Marcel Dekker, Inc., New York, NY, 2001.
[8] D.D. McLaren, R.G. Hollenbeck, Drug Dev. Ind. Pharm. 13 (1987) 2179–2197.

[9] Y. Mouget, P. Gosselin, M. Tourigny, S. Béchard, Am. Lab. 35 (2003) 20–22.
[10] L. St-Onge, E. Kwong, M. Sabsabi, E.B. Vadas, Spectrochim. Acta, Part B 57 (2002) 1131–1140.
[11] J.D. Kirsch, J.K. Drennen, J. Pharm. Biomed. Anal. 13 (1995) 1273–1281.
[12] J.D. Kirsch, J.K. Drennen, Pharm. Res. 13 (1996) 234–237.
[13] M. Anderson, M. Josefson, F. Langkilde, K.-G. Wahlund, J. Pharm. Biomed. Anal. 20 (1999) 27–37.
[14] M. Anderson, S. Folestad, J. Gottfries, M.O. Johansson, M. Josefson, K.-G. Wahlund, J. Anal. Chem. 72 (2000) 2099–2108.
[15] S. Romero-Torres, J.D. Pérez-Ramos, K.R. Morris, E.R. Grant, J. Pharm. Biomed. Anal. 38 (2005) 270–274.
[16] J.D. Pérez-Ramos, W.P. Findlay, G. Peck, K.R. Morris, AAPS PharmSciTech 6 (2005) 127–136.
[17] B.M. Wise, N.B. Gallagher, R. Bro, J.M. Shaver, PLS_Toolbox 3.0 Manual, Manson, WA, 2003.
[18] P. Geladi, B.R. Kowalski, Anal. Chim. Acta 185 (1986) 1–17.
[19] R.G. Brereton, Chemometrics: Data Analysis for the Laboratory and Chemical Plant—The Solutions and Data Sets, Wiley, University of Bristol, Bristol, UK, 2002.
[20] S.E.J. Bell, J.R. Beattie, J.J. McGarvey, K.L. Peters, N.M.S. Sirimuthu, S.J. Speers, J. Raman Spectrosc. 35 (2004) 409–417.
[21] A. Savitzky, M.J.E. Golay, J. Anal. Chem. 36 (1964) 1627–1639.
[22] R.J. Barnes, M.S. Dhanoa, S.J. Lister, Appl. Spectrosc. 43 (1989) 772–777.
[23] O. Svensson, M. Josefson, F.W. Langkilde, Chemom. Intell. Lab. Syst. 49 (1999) 49–66.
[24] P. Geladi, D. MacDougall, H. Martens, Appl. Spectrosc. 39 (1985) 491–500.
[25] M.S. Dhanoa, S.J. Lister, R. Sanderson, R.J. Barnes, J. Near Infrared Spectrosc. 2 (1994) 43–47.
[26] K.H. Esbensen, Multivariate Data Analysis in Practice, fifth ed., Camo, Aalborg University, Esbjerg, 2002.
[27] D. Zhang, D. Ben-Amotz, Appl. Spectrosc. 54 (2000) 1379–1383.